

A 3-D Integrator-Differentiator Double-Loop (IDD) Filter for Raster-Scan Video Processing

R. K. Bertschmann, N. R. Bartley and L. T. Bruton

Abstract— A novel RC-active circuit is proposed for the selective filtering of moving objects in raster-scanned analog video signals on the basis of their velocities. It consists of a feedforward continuous-time integrator and a two feedback loops with discrete-time differentiators in each loop. It has a frequency-planar passband in the 3-D space-time frequency domain.

I. INTRODUCTION

TWO-DIMENSIONAL (2-D) RC-active recursive filters having direct-form structures have been proposed [1]-[3] for the direct processing of raster-scanned video signals. It has been shown that such filters are naturally suited to the processing of raster-scanned signals in real time and that the hardware implementation is generally much easier than in pure-digital filter implementations.

In this contribution, we describe a *three-dimensional* (3-D) RC-active recursive filter circuit for the processing of raster-scanned video signals. This circuit is derived from a ladder-form implementation of a first-order 3-D recursive Linear-Trajectory (LT) filter [4]-[8]. The circuit, which is less complex than the direct-form realization [1]-[3], consists of a continuous-time feedforward integrator (*I*) and two discrete-time feedback differentiators (*D*) in a double-loop (*D*) and is referred to here as the 3-D Integrator-Differentiator Double-Loop (IDD) circuit.

The signal-flow graph (SFG) of the proposed 3-D IDD filter circuit is derived from a passive 3-D continuous-domain prototype LR filter [4]-[8]. We briefly review the required passive LR filter prototype network in Section II. In Section III, we review raster-scanned signals and how they may be represented as 3-D mixed-domain signals. A suitable mixed-domain SFG is described in Section IV, which is obtained from the LR prototype filter network by means of elemental predistortion techniques [5],[6], followed by bilinear transformation. The RC-active 3-D IDD circuit is described in Section V along with experimental verification of the 3-D frequency response. The space-time performance of the circuit is briefly summarized in Section VI.

II. REVIEW OF 3-D LT FILTERS

MD continuous-domain prototype filters, comprised of inductive, capacitive and resistive elements, have been used

R. K. Bertschmann is with Philips, Zürich, Switzerland; N. R. Bartley and L. T. Bruton are with the Department of Electrical and Computer Engineering, University of Calgary, Calgary, Alberta, Canada T2N 1N4. Contact author: L. T. Bruton.

The authors gratefully acknowledge the financial support of Micronet, the Federal Centre of Excellence on Microelectronic Devices, Circuits and Systems and the Natural Sciences and Engineering Research Council of Canada.

as the basis for realizable filter structures [4]-[8]. The 3-D continuous-domain LT LR filter network shown in Fig. 1 possesses frequency-domain characteristics which make it useful for enhancing 3-D LT signals. The 3-D magnitude

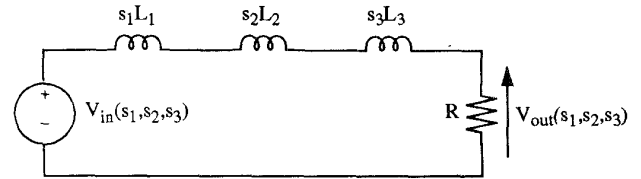


Fig. 1. A 3-D LT LR network

frequency response $M(\omega_1, \omega_2, \omega_3) = T(j\omega_1, j\omega_2, j\omega_3)$ is given by

$$M(\omega_1, \omega_2, \omega_3) = \frac{R}{\sqrt{R^2 + (\omega_1 L_1 + \omega_2 L_2 + \omega_3 L_3)^2}} \quad (1)$$

$M(\omega_1, \omega_2, \omega_3)$ has a resonant plane given by

$$\omega_1 L_1 + \omega_2 L_2 + \omega_3 L_3 = 0 \quad \text{Resonant Plane} \quad (2)$$

and has -3dB planes given by

$$\omega_1 L_1 + \omega_2 L_2 + \omega_3 L_3 = \pm R. \quad \text{-3dB Planes} \quad (3)$$

The resonant plane passes through the origin and has unit normals \mathbf{n} given by

$$\mathbf{n} = \frac{\pm 1}{\|\mathbf{L}\|_2} (e_1 L_1 + e_2 L_2 + e_3 L_3), \quad L_1, L_2, L_3 \geq 0 \quad (4)$$

where $\|\mathbf{L}\|_2 = \sqrt{L_1^2 + L_2^2 + L_3^2}$ and e_1, e_2 , and e_3 are the orthogonal unit basis vectors in the $\omega_1, \omega_2, \omega_3$ directions. The perpendicular distance between the resonant and -3dB planes is $R/\|\mathbf{L}\|_2$ and the 3-D Q-factor is defined in [4] as $Q = \|\omega\|_2 \|\mathbf{L}\|_2 / R$, where $\|\omega\|_2 = \sqrt{\omega_1^2 + \omega_2^2 + \omega_3^2}$.

III. RASTER-SCANNED VIDEO SIGNALS

Raster-scanning refers to the scanning of static 2-D images along closely spaced horizontal lines. This process is currently employed in commercial television systems such as that defined by the National Television Standards Committee (NTSC) [9]. In the NTSC standard, each static 2-D image, or *frame*, consists of 525 horizontal lines divided into two interlaced *fields*, one even and one odd, as shown in Fig. 2. The raster-scanning process in each frame

scans the 262.5 odd-numbered lines, corresponding to the odd field, followed by the 262.5 even-numbered lines, corresponding to the even field. Frames are scanned in this way at the rate of 30 frames per second. The filter described in Sections IV and V processes each frame in exactly this sequence, or equivalently, as the vertical concatenation of the odd and even fields.

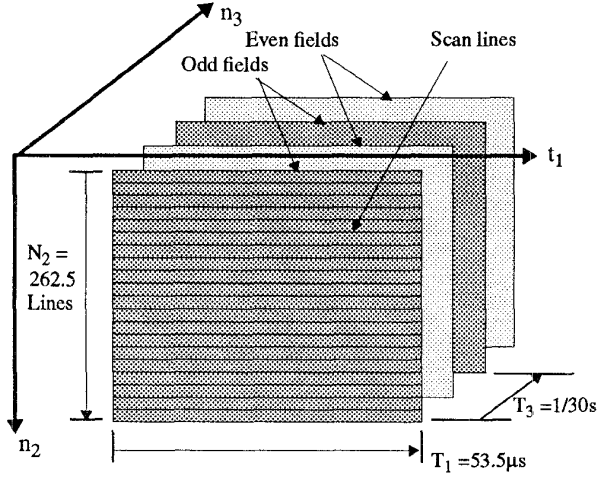


Fig. 2. An interlaced NTSC image sequence

Two consecutive lines of the raster-scanned video signal, as typically obtained from a scanning device such as a television camera, are shown in Fig. 3. This signal is *continuous-domain* in the row dimension t_1 ; that is, $t_1 \in [0; T_1]$, $t_1, T_1 \in \mathbb{R}^1$, where $T_1 = 53.5 \mu s$. At the end of the line, a horizontal synchronization pulse indicates that scanning is to begin on the next horizontal line. Thus, the raster-scanned video signal is *discrete-domain* in the column variable n_2 ; i.e., $n_2 \in [0; N_2]$, $n_2, N_2 \in \mathbb{N}^1$, where $N_2 = 525$ lines. Similarly, vertical synchronization pulses are inserted at the completion of each field and frames are counted after the completion of every even field. Thus, the raster-scanned video signal is also *discrete-domain* in the temporal variable n_3 ; i.e., $n_3 \in [0; \infty] \in \mathbb{N}^1$. The corresponding scanned 3-D image may therefore be represented as a 3-D mixed-domain signal $x(t_1, n_2 T_2, n_3 T_3)$ having domain $d_{mn}[x(t_1, n_2 T_2, n_3 T_3)] \in \mathbb{R}^1 \times \mathbb{N}^2$, where $T_2, T_3 \in \mathbb{R}^1$ are the column and temporal sample intervals, respectively.

IV. MIXED-DOMAIN LADDER-FORM SFG OF THE 3-D LT FILTER

In the field of 1-D signal processing, SFG simulation of LCR ladder filters has received a great deal of attention [10]-[12]. The extension of this work to the field of M-D signal processing has recently been explored [5],[6]. In [5],[6], the authors investigate the design of 3-D discrete-domain ladder-form structures from prototype 3-D LCR networks corresponding to LT filters and Plane-Wave (PW) filters. They propose a technique of elemental predistortion for obtaining *realizable* 3-D discrete-domain SFGs using the bilinear transformation. We propose to modify this technique

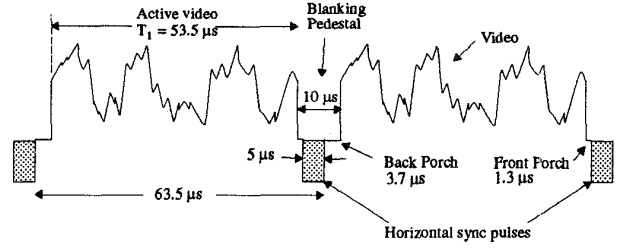


Fig. 3. Two lines from a raster-scanned video signal

here to obtain a realizable 3-D mixed-domain ladder-form SFG suitable for processing raster-scanned signals.

The proposed predistorted LR prototype network, corresponding to Fig. 1, is shown in Fig. 4. As shown, negative resistances $-r_2$ and $-r_3$ have been placed in series with the immittances $s_2 L_2$ and $s_3 L_3$, respectively. The input-output Laplace transform voltage transfer function $T(s_1, s_2, s_3)$ is clearly unaltered by these predistortions by the introduction of positive compensating resistances r_2 and r_3 in series with the terminating resistance R , as shown in Fig. 4.

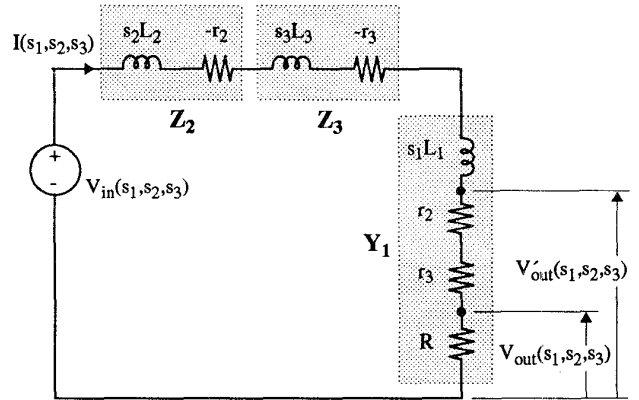


Fig. 4. The predistorted 3-D LR network

A simple Type I SFG [5][12] corresponding to the predistorted network in Fig. 4 is obtained, after some manipulation, and is shown in Fig. 5. This SFG contains a lossy integrating branch Y_1 having branch transmittance $b_1(s_1)$, as indicated, and two lossy differentiating branches Z_2, Z_3 having branch transmittances $b_2(s_2)$ and $b_3(s_3)$, also as indicated. Note that the output node in Fig. 5 is $V'_{out}(s_1, s_2, s_3)$, which is the voltage shown in Fig. 4. This differs from the desired $V_{out}(s_1, s_2, s_3)$ only by a constant scaling factor α , where $V'_{out}(s_1, s_2, s_3) = \alpha V_{out}(s_1, s_2, s_3)$ and $\alpha = (R + r_2 + r_3)/R$.

The mixed-domain SFG is obtained from the predistorted continuous-domain SFG in Fig. 5 by applying the bilinear transformation to the transmittances $b_2(s_2)$ and

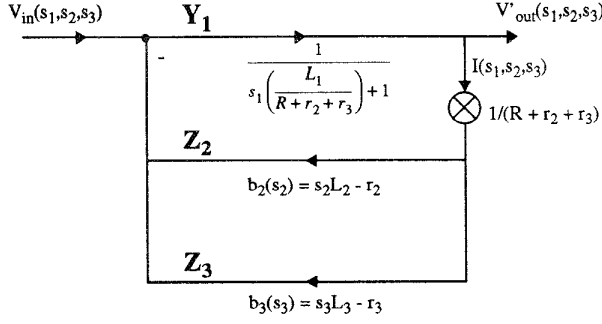


Fig. 5. Type I SFG of the predistorted LR network

$b_3(s_3)$ according to

$$b_i(z_i) = b_i(s_i) \Big|_{\frac{z_i - 1}{T_i}}^{\frac{z_i + 1}{T_i}} = \frac{2L_i z_i - 1}{T_i z_i + 1} - r_i, \quad i = 2, 3 \quad (5)$$

We choose

$$-r_i = -\frac{2L_i}{T_i} \quad i = 2, 3 \quad (6)$$

so that equation (5) simplifies to

$$b_i(z_i) = -\frac{4L_i}{T_i} \frac{1}{z_i + 1}, \quad i = 2, 3 \quad (7)$$

Each of $b_i(z_i)$, $i=2,3$ in equation (7) is easily implemented in the resulting mixed-domain SFG *without a delay-free forward path* [5].

Following the bilinear transformation of $b_2(s_2)$ and $b_3(s_3)$ in this way, it is necessary to scale s_1 in branch $b_1(s_1)$ in an equivalent way in order to restore the correct passband orientation in the resulting mixed-domain filter. For this, it is appropriate to use ks_1 where

$$k = \frac{T_{avs}}{N_1} \quad (8)$$

where $T_{avs} = \frac{3}{4}T_1 = 40.125\mu s$ is the aspect ratio-corrected portion of each scan line and $N_1 = 243$ is the number of visible lines in each field. This performs the equivalent scaling operation to sampling N_1 pixels in each continuous-domain raster-scan line in T_{avs} seconds.

The final mixed-domain SFG is shown in Fig. 6 and has an input-output voltage transfer function given by

$$T(s_1, z_2, z_3) = \frac{R + r_2 + r_3}{R + \frac{T_{avs}}{N_1} s_1 L_1 + \sum_{i=2}^3 \frac{2}{T_i} \frac{z_i - 1}{z_i + 1} L_i} \quad (9)$$

and a frequency response given by

$$T(j\omega_1, j\Omega_2, j\Omega_3) = \frac{R + r_2 + r_3}{R + j \frac{T_{avs}}{N_1} \omega_1 L_1 + \sum_{i=2}^3 j \frac{2}{T_i} \tan(\frac{\Omega_i}{2}) L_i} \quad (10)$$

V. THE 3-D IDD RC-ACTIVE CIRCUIT REALIZATION

The mixed-domain 3-D IDD SFG in Fig. 6 has been implemented using the simple RC-active 3-D IDD circuit

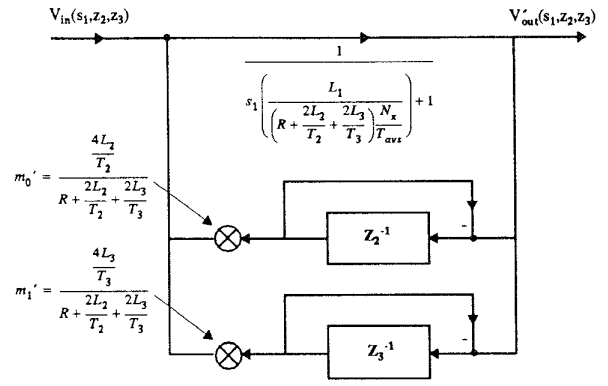


Fig. 6. The mixed-domain SFG of the 3-D IDD filter

shown in Fig. 7. The circuit employs wide-bandwidth operational amplifiers (GBW = 100MHz) along with a digitally sampled row delay and frame delay. The row and frame delays, for the discrete-time differentiators, have been constructed using 8-bit video A/D and D/A converters and they each buffer digitized video data through high-speed static RAM. The row delay z_2^{-1} samples at a rate of 12.1 MHz (or 768 samples per line) and achieves a row delay of precisely 63.5 μs . The frame delay z_3^{-1} samples at a rate of 7.86 MHz (or 262144 samples per frame) and achieves a frame delay of precisely 1/30 s.

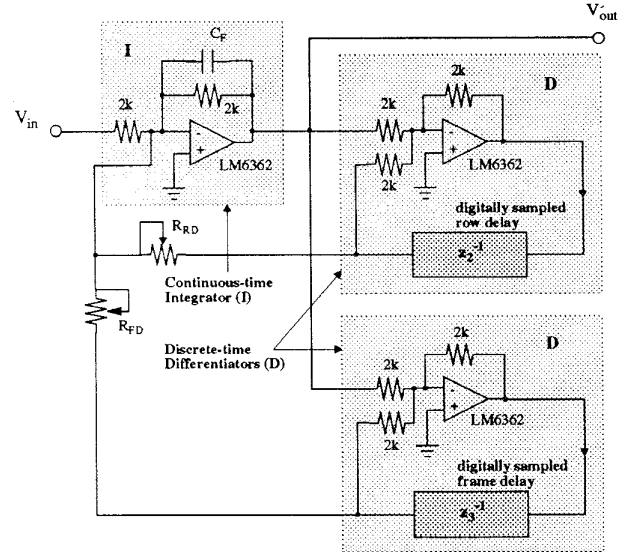


Fig. 7. The proposed RC-active 3-D IDD circuit

We have designed and implemented a 3-D IDD mixed-domain LT filter with $L_1 = 12$, $L_2 = 2.5$, $L_3 = 9$, and $R = 1$, corresponding to a 3-D Q-factor [4] of $Q = 15.21||\omega||_2$, and using the normalized bilinear transformation with $T_2 = T_3 = 1$. The component values in the circuit of Fig. 7 are $R_{FD} = 1333\Omega$, $R_{RD} = 4800\Omega$, and $C_F = 41.28pF$.

To experimentally verify the 3-D frequency response of

the 3-D LT IDD circuit, dynamic analog gray-scale 3-D sinusoidal images have been generated and displayed on a CRT screen. A television camera has been focused on the CRT display and used to obtain the composite video raster-scan input signal V_{in} to the 3-D IDD circuit. The amplitudes of the sinusoidal input and output raster-scan signals have been carefully measured to determine the gain frequency response $M(k\omega_1, \Omega_2, \Omega_3)$ of the filter.

The resonant plane for this filter, from (10), is given by

$$\frac{T_{avs}}{N_1} \omega_1 L_1 + 2 \tan\left(\frac{\Omega_2}{2}\right) L_2 + 2 \tan\left(\frac{\Omega_3}{2}\right) L_3 = 0 \quad (11)$$

This plane is shown as a surface plot in Fig. 8. Also shown in Fig. 8 are lines L_1 and L_2 that are parallel to the Ω_3 axis and intersect the resonant plane at points P_1 and P_2 , respectively. Gain frequency response measurements have been taken along one such line, L_1 , and are shown with the calculated response in Fig. 9. As shown, the measured peak accurately aligns with the point P_1 and the roll-off confirms the selectivity of the filter, within measurement error. Although not shown here, similar results have been obtained along line L_2 .

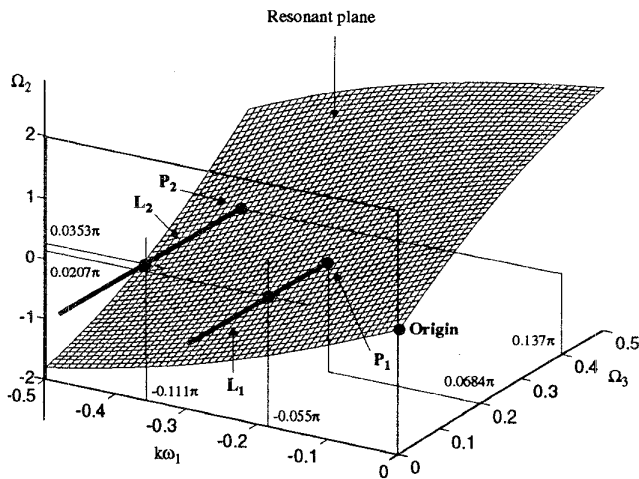


Fig. 8. Frequency response of mixed-domain 3-D LT filter

VI. EXPERIMENTAL SPACE-TIME PERFORMANCE

Experimental verification of the space-time response of the circuit has been obtained, but is omitted for brevity. A moving passband object, having a space-time linear trajectory of (1.33, 0.28) pixels per frame, has been processed using Fig. 7 and the displayed NTSC raster-scan output V'_{out} is a good video replica of the input. When the trajectory of the object is altered to a stopband value, for example to (-1.33, 0.28) pixels per frame, the output object is significantly attenuated.

VII. CONCLUSION

An analog RC-active circuit is proposed using a continuous-time feedforward integrator and two discrete-time feed-

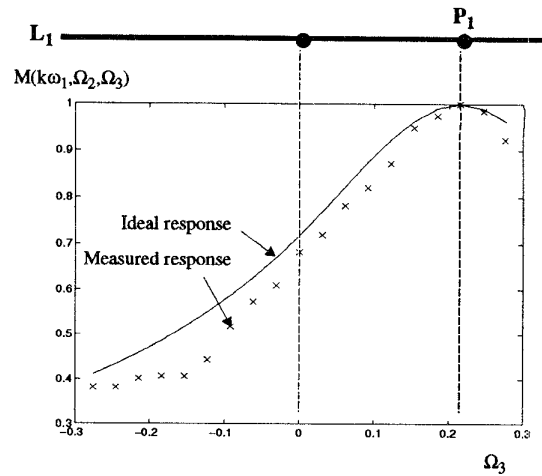


Fig. 9. Measured and actual frequency response along L_1

back differentiators. This 3-D IDD circuit selectively enhances moving objects in raster-scanned video signals if the objects have specific velocities that correspond to the orientation of the frequency-planar passband. Objects having other velocities are in the stopband and are appropriately attenuated. To our knowledge, this is the first real-time 3-D recursive filter that has been reported in the literature.

REFERENCES

- [1] M. A. Sid-Ahmed, "Two-Dimensional Analog Filters: A New Form of Realization," *IEEE Trans. on Circuits and Systems*, Vol. CAS-36, No. 1, pp. 153-154, January 1989.
- [2] M. A. Sid-Ahmed et al, "Method and an Apparatus for 2-D Filtering a Raster Scanned Image in Real Time," United States Patent 5,122,788, June 16, 1992.
- [3] H. J. Kaufman and M. A. Sid-Ahmed, "2-D Analog Filters for Real Time Video Signal Processing," *IEEE Trans. on Consumer Elect.*, Vol. 36, No. 2, pp. 138-141, May 1990.
- [4] L. T. Bruton and N. R. Bartley, "Three-Dimensional Image Processing Using the Concept of Network Resonance," *IEEE Trans. on Circuits and Systems*, Vol. CAS-32, No. 7, pp. 664-672, July 1985.
- [5] Y. Zhang and L. T. Bruton, "Differentiator-Type Three-Dimensional Recursive Ladder Filters Having Frequency-Planar- or Frequency-Beam-Shaped Passbands," *IEEE Trans. on Circuits and Systems for Video Technology*, Vol. CSVT-2, No. 3, pp. 297-304, September 1992.
- [6] Y. Zhang and L. T. Bruton, "Applications of 3-D LCR networks in the design of 3-D recursive filters for processing image sequences," *IEEE Trans. on Circuits and Systems for Video Technology*, Vol. CSVT-4, No. 4, pp. 369-382, August 1994.
- [7] Q. Liu and L. T. Bruton, "Design of 3-D Planar and Beam Digital Filters using Spectral Transformations," *IEEE Trans. on Circuits Systems*, Vol. CAS-36, No. 3, March 1989.
- [8] L. T. Bruton and N. R. Bartley, "Highly-selective Three-dimensional Recursive Beam Filters using Intersecting Resonant Planes," *IEEE Trans. on Circuits and Systems*, Vol. CAS-30, No. 3, March 1983.
- [9] A. A. Liff, *Color and Black and White Television Theory and Servicing*, Englewood Cliffs, NJ: Prentice Hall, 1985.
- [10] A. S. Sedra and P.O. Brackett, *Filter Theory and Design: Active and Passive*, Beaverton, Oregon: Matrix Publishers, 1978.
- [11] R. Schauman, M. S. Ghausi and K. R. Laker, *Design of Analog Filters*, Englewood Cliffs, NJ: Prentice-Hall, 1990.
- [12] L. T. Bruton, "Low-Sensitivity Digital Ladder Filters," *IEEE Trans. on Circuits and Systems*, Vol. CAS-22, No. 3, pp. 168-175, March 1975.
- [13] L. T. Bruton, *RC-Active Circuits*, Englewood Cliffs, NJ: Prentice-Hall, 1980.